Progress In Electromagnetics Research C, Vol. 84, 135–145, 2018

Single-Fed Low-Profile Circularly Polarized Antenna Using Quarter-Mode Substrate Integrated Waveguide with Enhanced Bandwidth

Ni Wang[1, *], Xiaowen Xu[1], and Murilo H. Seko[2]

Abstract—A single-fed compact circularly polarized quarter-mode substrate integrated waveguide (QMSIW) antenna with improved bandwidth is designed based on a single-layer structure. The antenna consists of four QMSIW elements. Instead of using a complex power divider to excite each element, an inset microstrip line is employed to excite the driven QMSIW element, while the parasitic QMSIW elements are excited by means of gap and direct couplings. Moreover, the phase and magnitude of the electromagnetic fields in each QMSIW element are controlled by gaps and short sections of microstrip line to obtain a circularly polarized radiation. A prototype of the proposed antenna is fabricated and measured, and the measured results are in good agreement with the simulated ones. The measured 10-dB impedance bandwidth is 6.23%, from 5.13 GHz to 5.46 GHz, and the 3-dB axial-ratio bandwidth is 3.62%, from 5.15 GHz to 5.34 GHz. The measured maximum gain of the antenna is 6.46 dBic.

1. INTRODUCTION

Circularly polarized (CP) antennas are extensively applied in satellite and wireless communication systems because of their ability to mitigate polarization mismatch and reduce multipath effects. Single-fed CP antennas are especially desired due to their simple configuration and ease of connection. On the other hand, the substrate integrated waveguide (SIW) has attracted great attention since it can benefit from the advantages offered by the waveguide and microstrip technologies, such as light weight, low profile, reduced losses, and ease of integration with planar circuits [1–6]. Aiming at the miniaturization of the SIW, three types of structures derived from the traditional SIW have been proposed: the half-mode substrate integrated waveguide (HMSIW) [6–11], which is achieved by cutting the SIW along its fictitious magnetic wall; the quarter-mode substrate integrated waveguide (QMSIW) [12–14], which is obtained by bisecting the HMSIW on its fictitious magnetic wall; and the eighth-mode substrate integrated waveguide (EMSIW) [15, 16], which is realized by splitting the QMSIW along its fictitious magnetic wall. An SIW antenna using a cross-shaped slot for obtaining CP radiation is presented in [1]. In this antenna, the cross-shaped slot, whose arms have different lengths, allows the excitation of two degenerate resonant modes that are orthogonal and 90° out of phase. The 3-dB axial-ratio (AR) bandwidth exhibited by this antenna is 0.8%. In [6], two single-fed cavity-backed slot CP antennas are investigated. The first one is based on the SIW using a spoon-shaped slot, and the second one is based on the HMSIW employing a semicircle slot. The 3-dB AR bandwidths of these antennas are 1.8% and 2.3%, respectively. By exciting two quarter-wavelength patch modes that are orthogonal to each other, a single-layer slot antenna using HMSIW is designed in [7] to produce CP radiation with a 3-dB AR bandwidth of 1.74%. A CP QMSIW antenna operating in a higher-order resonant mode that exhibits

Received 10 April 2018, Accepted 17 May 2018, Scheduled 30 May 2018

* Corresponding author: Ni Wang (wangnibit@gmail.com).

[1] School of Information and Electronics, Beijing Institute of Technology, Beijing 100081, People's Republic of China. [2] Department of Electronic Systems Engineering, Polytechnic School, University of Sao Paulo, Sao Paulo 05508-010, Brazil.

a 3-dB AR bandwidth of 2.79% is proposed in [12]. A compact broadband CP antenna consisting of four EMSIW cavities fed by a power divider through four probes is presented in [15]. The use of such a feeding network requires dual-layer PCB fabrication techniques, which is more complex and leads to a higher fabrication cost. Besides that, the use of a power divider increases the losses of the antenna. Therefore, a single-fed CP antenna with increased AR bandwidth is desirable for several applications.

This paper proposes a single-fed low-profile antenna with broader CP bandwidth using QMSIW technology. Gaps and short sections of microstrip line are used in this antenna to control the phase and magnitude of the electromagnetic fields in each QMSIW element with the aim of generating CP radiated waves. The measured results of the presented antenna demonstrate a 10-dB impedance bandwidth of 6.23% (5.13–5.46 GHz), and a 3-dB axial-ratio bandwidth of 3.62% (5.15–5.34 GHz) with a maximum gain of 6.46 dBic. Therefore, this antenna is suitable for portable devices that operate in IEEE 802.11a (5.15–5.35 GHz) WLAN systems.

2. LINEARLY POLARIZED QMSIW ANTENNA DESIGN

A linearly polarized (LP) antenna is presented based on the QMSIW, which is derived from the square SIW. The evolution of the QMSIW cavity is illustrated in Fig. 1 with the aid of the simulated electric-field distributions obtained using ANSYS HFSS. Due to the large width-to-height ratio of the SIW, only TM modes can be supported in the cavity. Considering the dominant mode of the SIW cavity, the magnetic field is perpendicular to the symmetrical planes, AA', BB', CC', and DD', which can be regarded as perfect magnetic walls, as shown in Fig. 1(a). The HMSIW cavity is realized by cutting the square SIW cavity along BB', and the QMSIW cavity is obtained by further bisecting the HMSIW cavity along OD', as shown in Fig. 1(b) and Fig. 1(c), respectively. It is observed that the electric field of the QMSIW cavity is almost the same as that of a one-quarter section of the original SIW cavity, and the size is reduced by 75% compared with the square SIW cavity. The resonance frequencies of the QMSIW cavity can be calculated using the following equation [17, 18]:

$$f_{mn0} = \frac{1}{2a_{eff}\sqrt{\mu\varepsilon}}\sqrt{m^2+n^2} \tag{1}$$

where m and n are integers, and $m \neq n$. $\mu = \mu_0\mu_r$ and $\varepsilon = \varepsilon_0\varepsilon_r$ are the permeability and permittivity of the substrate, respectively. The parameter a_{eff} is the equivalent length [19, 20] of the cathetus of the QMSIW cavity and can be determined by the expression below:

$$a_{eff} = \frac{\sqrt{2}}{2}W_{eff}^{SIW} \tag{2}$$

$$W_{eff}^{SIW} = (2L_c) - 1.08\frac{d^2}{s} + 0.1\frac{d^2}{(2L_c)} \tag{3}$$

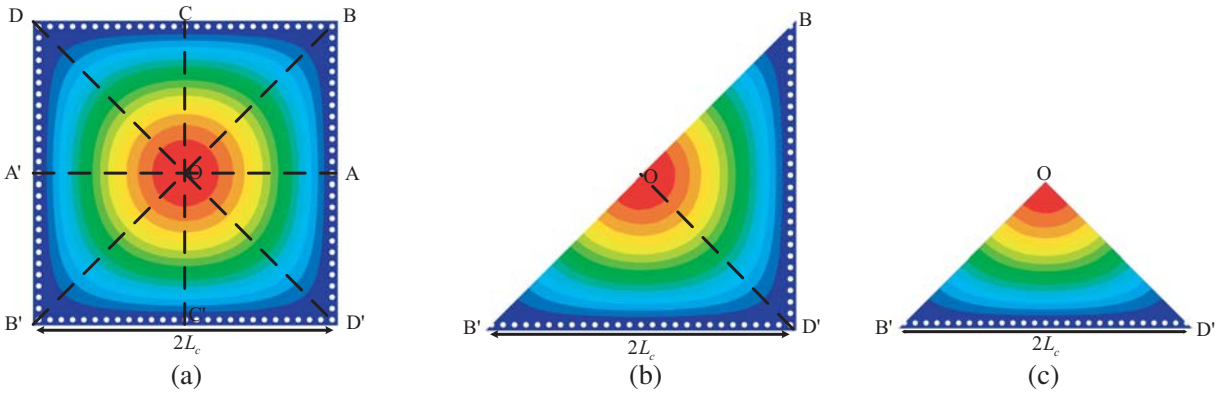

Figure 1. Simulated electric-field distributions for the dominant mode of the (a) square SIW cavity, (b) HMSIW cavity, (c) QMSIW cavity.

where W_{eff}^{SIW} is the length of the equivalent conventional waveguide cavity that has the same resonance frequencies as an SIW cavity with side length $2L_c$. The values d and s are the via-hole diameter and the distance between adjacent via holes, respectively. Because of the fringing fields along the two open sides of the QMSIW cavity, the actual resonance frequencies are slightly lower than the ones calculated by using (1).

The geometry of the designed microstrip line inset-fed LP antenna based on the QMSIW cavity is shown in Fig. 2. A dielectric substrate using Rogers RT/Duroid 5880 laminate (dielectric constant $\varepsilon_r = 2.2$ and loss tangent $\tan\delta = 0.0009$) with a thickness of 1.575 mm is chosen for the design of this antenna. A metal via-hole array is used to practically implement the electric wall required by the QMSIW cavity in the microstrip structure. The mentioned via holes are 0.5 mm in diameter d, and the distance s between the centers of two neighbouring via holes within a via-hole row is 1 mm. The distance between the hypotenuse of the QMSIW cavity and the centers of the via holes v is 0.5 mm. The side of the single QMSIW element a_s is 18.05 mm in length. Other parameters of the antenna are $w_{f_s} = 3.01$ mm, $P_s = 30.75$ mm, $P_{f_s} = 17.99$ mm, $P_{3_s} = 0.6$ mm, and $P_{4_s} = 1.69$ mm and are indicated in Fig. 2. The simulated reflection coefficient of the designed LP antenna is plotted in Fig. 3. As can be seen, this antenna resonates at 5.25 GHz, and the resonance corresponds to the TM_{010}/TM_{100} mode of the QMSIW cavity.

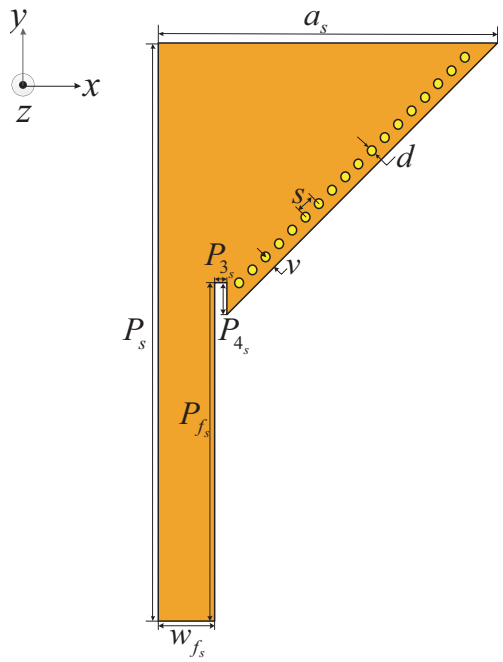

Figure 2. Configuration of the designed LP antenna.

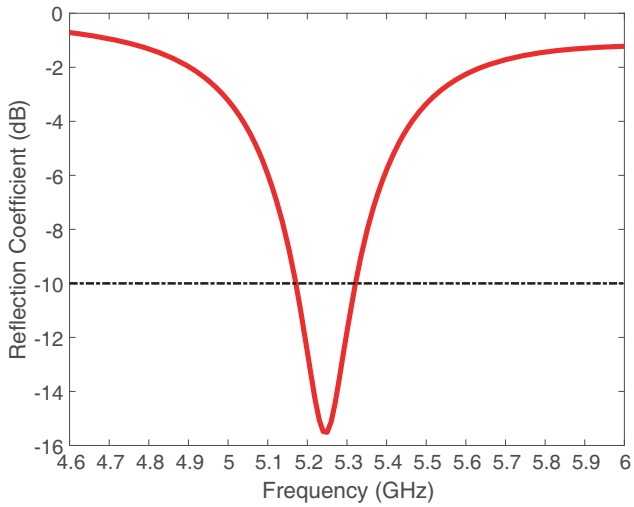

Figure 3. Simulated reflection coefficient of the designed LP antenna.

3. CIRCULARLY POLARIZED QMSIW ANTENNA DESIGN

A compact CP antenna can be designed depending on the small size of the proposed LP antenna. The configuration of the designed CP antenna is shown in Fig. 4. This antenna can produce two orthogonal radiated field components due to the sequential 90° rotation of its four QMSIW cavities. The dominant TM_{010}/TM_{100} mode in the driven QMSIW element is excited by means of an inset microstrip line, similarly to the designed LP antenna. Four QMSIW elements are gap coupled and directly connected to each other using the same gap width and different short sections of microstrip line. By adjusting the gap width between the elements of this antenna and the lengths of these microstrip line sections, the same magnitude for the two orthogonal field components and a 90° phase difference between the

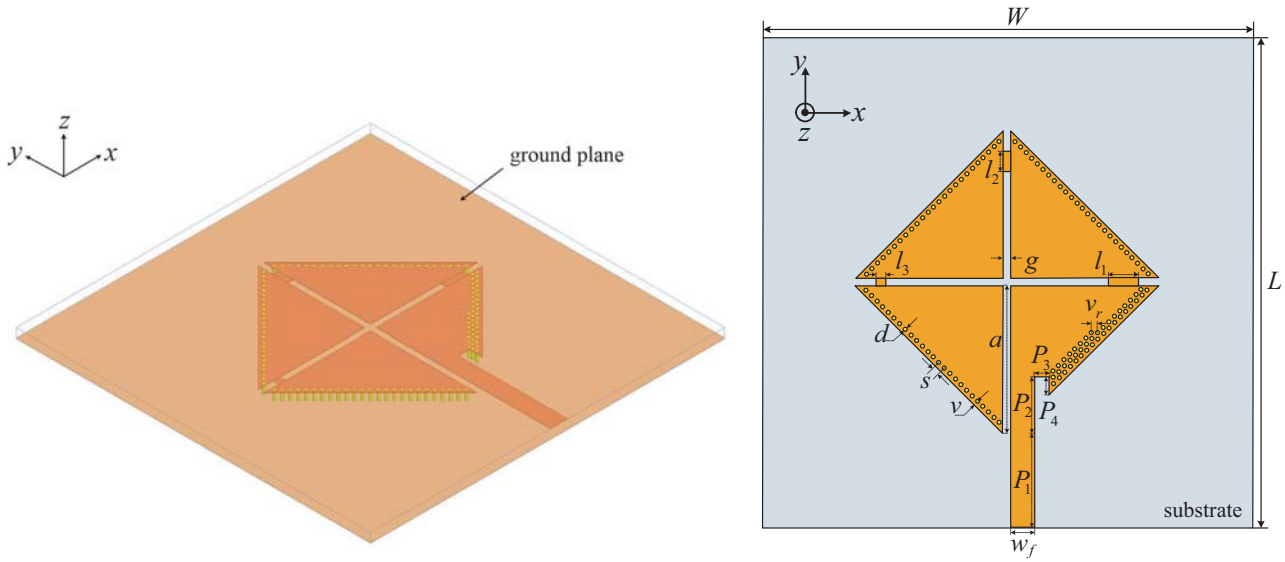

(a) (b)

Figure 4. Configuration of the designed CP antenna. (a) 3D view. (b) Top view.

fields excited in each element, sequentially, can be obtained. The same dielectric substrate employed by the presented LP antenna (Rogers RT/Duroid 5880 with thickness 1.575 mm) is used to design the CP antenna. The via-hole parameters are $d = 0.5$ mm, $s = 1$ mm, and $v = 0.5$ mm. The horizontal distance v_r between the centers of each row of via holes in the driven QMSIW element is 0.71 mm. The side of each QMSIW element a is 18.8 mm in length. The gap between adjacent QMSIW elements g is 1 mm. The lengths of the three short sections of microstrip line are $l_1 = 3.8$ mm, $l_2 = 2.6$ mm, and $l_3 = 1.2$ mm. The parameters of the inset microstrip line are $w_f = 3.01$ mm, $P_1 = 11.95$ mm, $P_2 = 7.3$ mm, $P_3 = 1.9$ mm, and $P_4 = 2.39$ mm. The substrate and the ground plane are equal in area with dimensions $L = W = 62.5$ mm.

In order to obtain a better impedance matching, two and a half rows of via holes are employed in the driven QMSIW cavity instead of just one. The insertion of additional rows of via holes on the

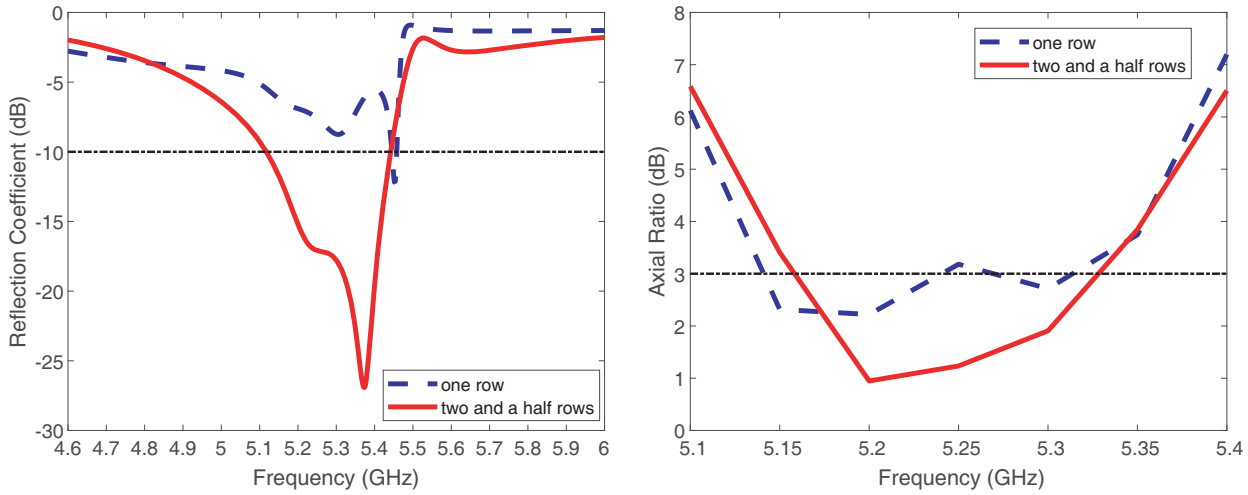

(a) (b)

Figure 5. Simulated reflection coefficient and AR for the two via-hole configurations in the proposed CP antenna. (a) Reflection coefficient. (b) AR.

hypotenuse changes the effective position of the electric wall implemented by the via holes. This wall is moved inwards with respect to the QMSIW patch, which reduces the size of the QMSIW cavity and approaches the electric wall to the feeding microstrip line, changing the input impedance of the antenna. Fig. 5 displays the simulated reflection coefficient and AR for these two via-hole configurations in the CP antenna. It is observed that an enhanced impedance bandwidth and CP radiation can be achieved for this antenna using two and a half rows of via holes.

The simulated surface current distributions on the designed CP antenna at 5.25 GHz for different phases are depicted in Fig. 6. Two orthogonal current distributions with equal magnitude and phase

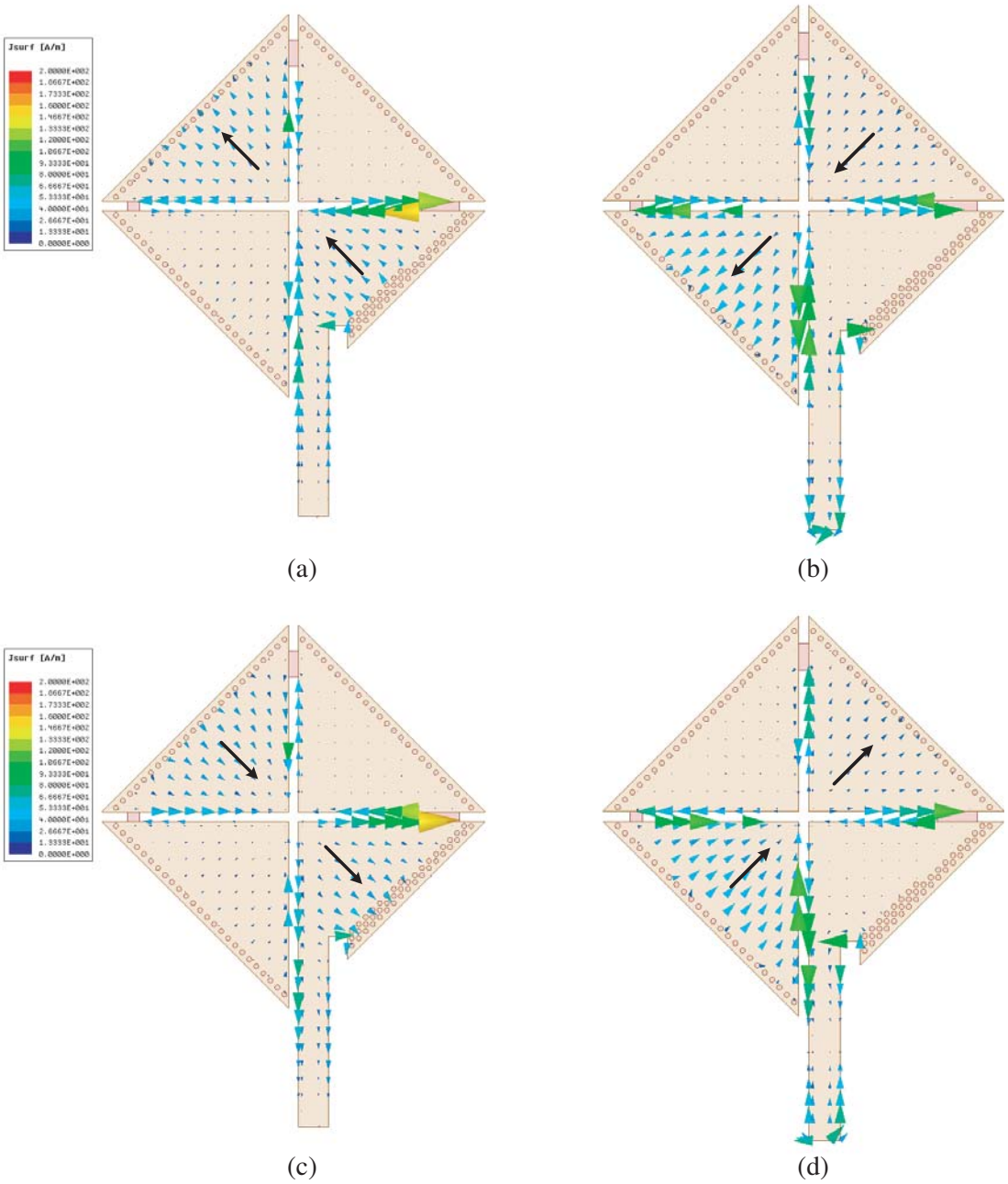

Figure 6. Simulated surface current distributions on the designed CP antenna at 5.25 GHz for different phases. (a) Phase = 0°. (b) Phase = 90°. (c) Phase = 180°. (d) Phase = 270°.

difference of 90° can be observed. The current rotates counterclockwise, which produces a right-handed (RH) CP radiation.

4. PARAMETRIC STUDIES

To investigate the impact of different geometric parameters on the performance of the proposed CP antenna, a set of parametric studies is carried out.

4.1. Effect of the Cathetus Length

The simulated reflection coefficient and AR for two different cathetus lengths of the proposed CP antenna (a) are illustrated in Fig. 7. The value $a = 18.05\,\text{mm}$ is the side length of the designed LP antenna at 5.25 GHz. When the catheti of the four QMSIW elements are equal to the value adopted for the LP antenna, the operating band of the CP antenna is shifted to a higher frequency range because of the mutual coupling between the elements. Therefore, a is optimized so that the CP antenna operates in the 5.25 GHz band, which leads to $a = 18.8\,\text{mm}$.

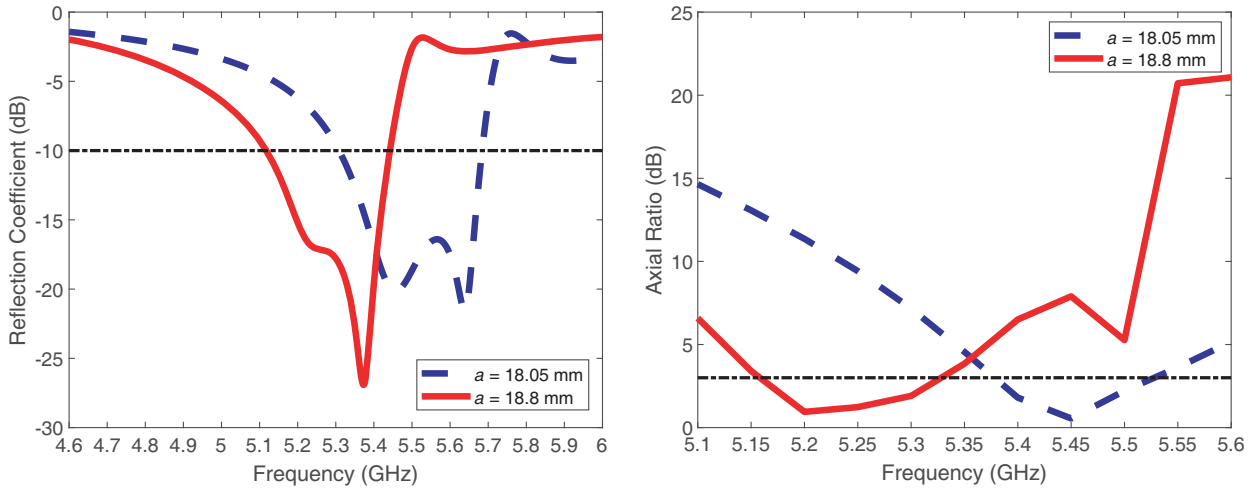

Figure 7. Simulated reflection coefficient and AR for different QMSIW cathetus lengths of the proposed CP antenna. (a) Reflection coefficient. (b) AR.

4.2. Effect of the Gap between the QMSIW Elements

The distance between QMSIW elements of the CP antenna controls the electromagnetic coupling between the mentioned elements and has a strong influence on the quality of the CP radiated field. For present antenna design, the same gap width is adopted between elements to keep the antenna symmetric. The simulated reflection coefficient and AR for different gap values g are shown in Fig. 8. It can be seen that the impedance bandwidth of the antenna is slightly affected by the gap width, while the AR is sensitive to this parameter. The value $g = 1\,\text{mm}$ is chosen for the CP antenna since it leads to the widest AR bandwidth and an acceptable impedance bandwidth.

4.3. Effect of the Ground Plane Size

Figure 9 shows the simulated reflection coefficient and AR for different ground plane sizes of the proposed CP antenna. The results of the simulated performance are summarized in Table 1. It can be observed that the larger the ground plane is, the larger the impedance bandwidth is, and the narrower the AR bandwidth is. It is worth mentioning that the operating bandwidth of a CP antenna is determined by

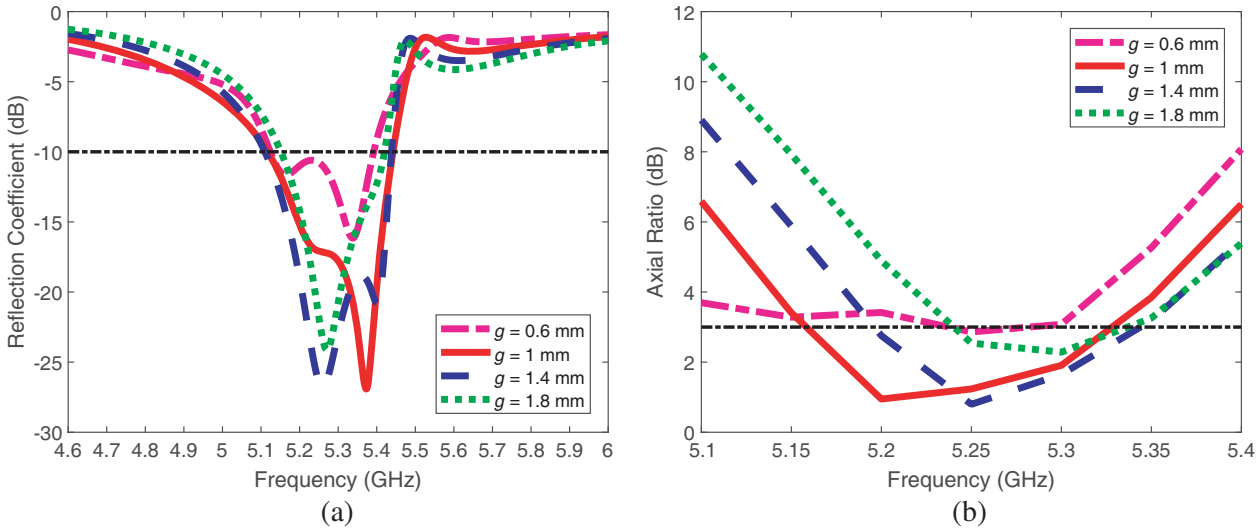

Figure 8. Simulated reflection coefficient and AR for different gap width g of the proposed CP antenna. (a) Reflection coefficient. (b) AR.

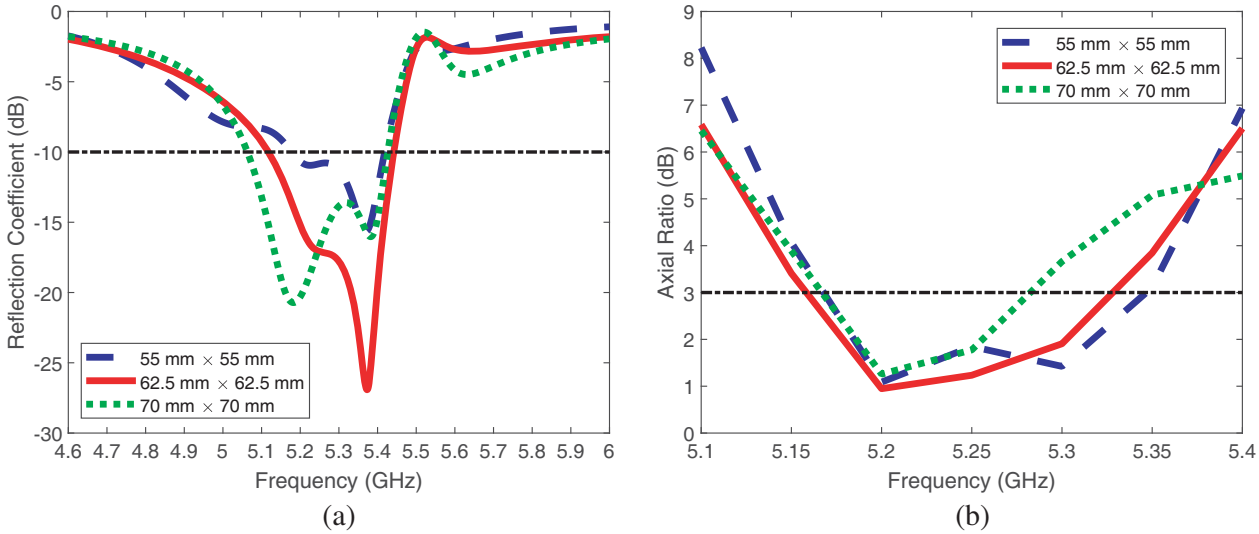

Figure 9. Simulated reflection coefficient and AR for different ground plane sizes of the proposed CP antenna. (a) Reflection coefficient. (b) AR.

Table 1. Simulated antenna performance for different ground plane sizes of the proposed CP antenna.

Ground plane size (mm^2)	10-dB impedance bandwidth (GHz)	3-dB AR bandwidth (GHz)	Bandwidth (GHz)
55×55	5.18–5.42 (4.53%)	5.17–5.35 (3.42%)	5.18–5.35 (3.23%)
62.5×62.5	5.11–5.44 (6.26%)	5.16–5.33 (3.24%)	5.16–5.33 (3.24%)
70×70	5.06–5.43 (7.05%)	5.17–5.28 (2.11%)	5.17–5.28 (2.11%)

both the impedance and AR bandwidths. A ground plane size of 62.5 mm × 62.5 mm is shown to lead to the widest bandwidth and, therefore, is chosen for the proposed CP antenna.

5. SIMULATED AND MEASURED RESULTS

A prototype of the designed CP antenna using QMSIW shown in Fig. 4 has been fabricated. Photographs of the fabricated antenna are presented in Fig. 10. The simulated and measured reflection coefficients of the designed CP antenna are plotted in Fig. 11. The experimental value for the 10-dB impedance bandwidth is 6.23%, obtained from 5.13 GHz to 5.46 GHz. Fig. 12 exhibits the simulated and measured AR results of the antenna in the broadside direction. The measured 3-dB AR bandwidth is 3.62%, obtained from 5.15 GHz to 5.34 GHz. Fig. 13 shows curves of the simulated and measured antenna gains in the broadside direction. The measured maximum gain within the 3-dB AR band is 6.46 dBic, and the measured gain at 5.25 GHz is 5.91 dBic. Slight differences between the simulated and measured results are observed, which can be attributed to the tolerances of the material properties and fabrication process. The simulated radiation efficiency of the designed CP antenna is also illustrated in Fig. 13. The maximum simulated radiation efficiency is 97.37% at 5.25 GHz, and the overall simulated radiation

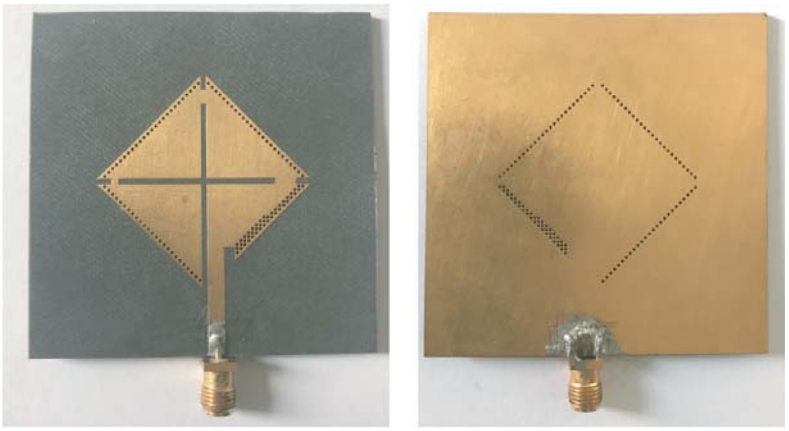

(a) (b)

Figure 10. Photographs of the fabricated CP antenna. (a) Top view. (b) Bottom view.

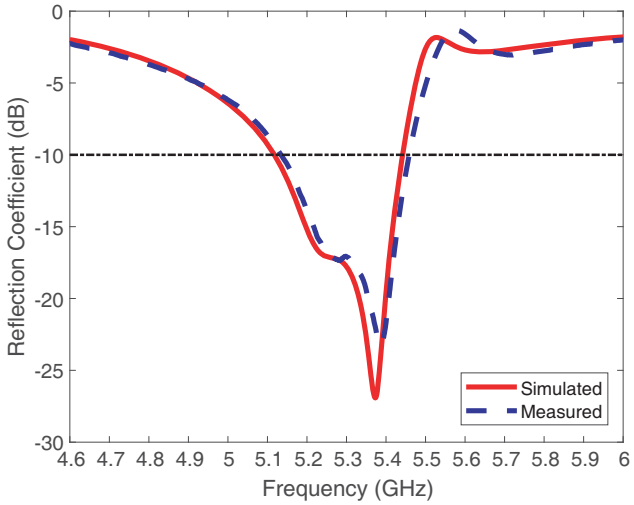

Figure 11. Simulated and measured reflection coefficients of the proposed CP antenna.

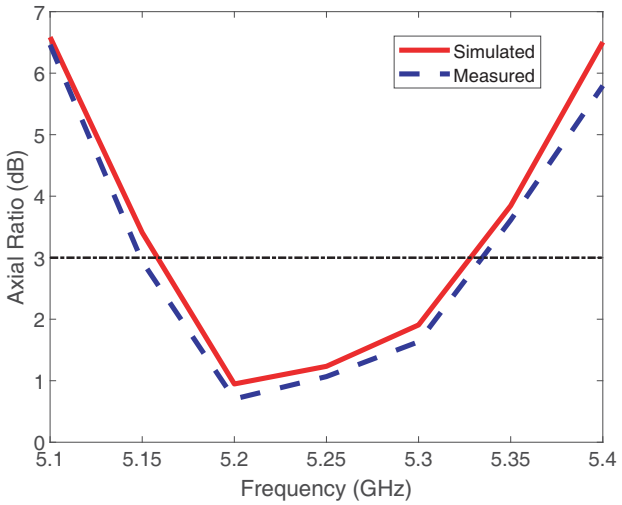

Figure 12. Simulated and measured ARs of the proposed CP antenna.

Table 2. Comparison between the performances of the proposed antenna and previously reported antennas.

Antenna	Technique	Frequency (GHz)	3-dB ARBW (%)	10-dB IBW (%)	Radiator area (λ_0^2)	Peak Gain (dBic)	Single -fed
[1]	SIW	10.1	0.8	2.8	0.312	6.3	Yes
[4]	SIW	10.3	2.3	18.74	0.731	5.75	Yes
[5]	SIW	6.57	0.99	3.2	0.504	9.6	Yes
[6]	SIW	28	1.8	6.3	0.332	5.9	Yes
[7]	HMSIW	8.67	0.66	6	0.101	4.2	Yes
[9]	HMSIW	10	2.2	11.9	0.275	6	Yes
[12]	QMSIW	10.8	2.79	21.6	0.259	7.13	Yes
[16]	EMSIW	1.645	0.61	1.82	0.056	0.7	No
This work	QMSIW	5.25	3.62	6.23	0.24	6.46	Yes

ARBW: Axial ratio bandwidth. IBW: Impedance bandwidth.

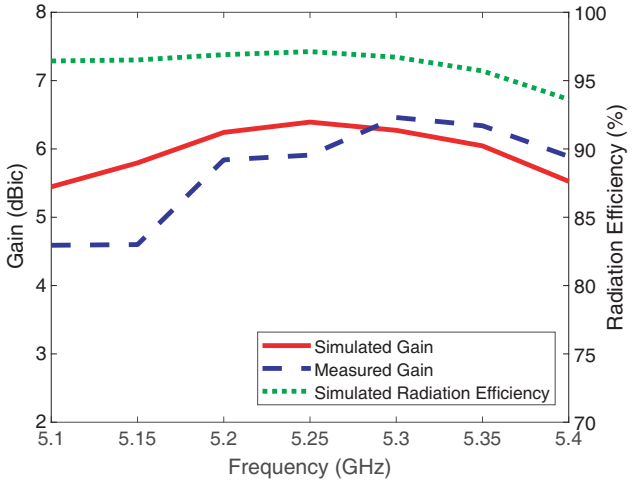

Figure 13. Simulated and measured gains and simulated radiation efficiency of the proposed CP antenna.

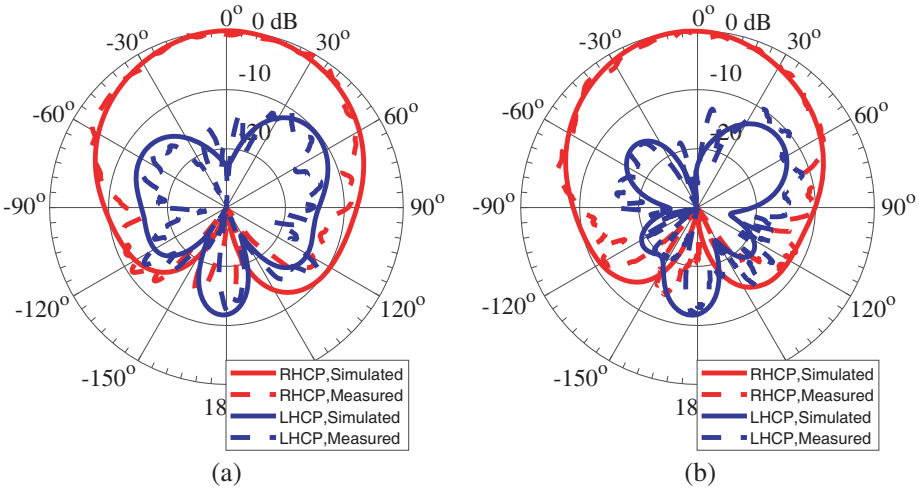

Figure 14. Simulated and measured normalized radiation patterns of the proposed CP antenna at 5.25 GHz. (a) xz-plane. (b) yz-plane.

efficiency is higher than 96.32% in the operating AR bandwidth. Fig. 14 plots the simulated normalized CP radiation patterns along with the measured ones for the xz-plane ($\phi = 0°$) and yz-plane ($\phi = 90°$) at 5.25 GHz.

A comparison between the performances of the proposed CP antenna and previously reported single-layer antennas is shown in Table 2. The radiator area of the antennas is related to the free space wavelength λ_0 at the corresponding resonance frequencies. It can be verified that the designed CP antenna can produce an improved AR bandwidth with small radiator area and moderate gain.

6. CONCLUSION

A single-fed compact CP antenna using QMSIW with increased bandwidth is proposed in this paper. Gaps and short microstrip line sections with different lengths interconnecting the QMSIW elements are used to obtain two radiated field components that are orthogonal, have the same magnitude, and are 90° out of phase for achieving CP radiation in a wider frequency band. The measured 10-dB impedance bandwidth of the antenna is 6.23%; the 3-dB AR bandwidth is 3.62%; the maximum gain is 6.46 dBic. Both the simulated and experimental results validate the designed antenna, which can be used either as a single antenna or as an array element.

REFERENCES

1. Luo, G., Z. Hu, Y. Liang, L. Yu, and L. Sun, "Development of low profile cavity backed crossed slot antennas for planar integration," *IEEE Trans. Antennas Propag.*, Vol. 57, No. 10, 2972–2979, 2009.
2. Bozzi, M., A. Georgiadis, and K. Wu, "Review of substrate-integrated waveguide circuits and antennas," *IET Microw., Antennas Propag.*, Vol. 5, No. 8, 909–920, 2011.
3. Wu, K., Y. Cheng, T. Djerafi, and W. Hong, "Substrate-integrated millimeter-wave and terahertz antenna technology," *Proceedings of the IEEE*, Vol. 100, No. 7, 2219–2232, 2012.
4. Kim, D., J. W. Lee, C. S. Cho, and T. K. Lee, "X-band circular ring-slot antenna embedded in single-layered SIW for circular polarisation," *Electron. Lett.*, Vol. 45, No. 13, 668–669, 2009.
5. Hao, Z., X. Liu, X. Huo, and K. Fan, "Planar high-gain circularly polarized element antenna for array applications," *IEEE Trans. Antennas Propag.*, Vol. 63, No. 5, 1937–1948, 2015.
6. Wu, Q., H. Wang, C. Yu, and W. Hong, "Low profile circularly polarized cavity-backed antennas using SIW techniques," *IEEE Trans. Antennas Propag.*, Vol. 64, No. 7, 2832–2839, 2016.
7. Razavi, S. A. and M. H. Neshati, "Development of a low-profile circularly polarized cavity-backed antenna using HMSIW technique," *IEEE Trans. Antennas Propag.*, Vol. 61, No. 3, 1041–1047, 2013.
8. Razavi, S. A. and M. H. Neshati, "Development of a linearly polarized cavity-backed antenna using HMSIW technique," *IEEE Antennas Wireless Propag. Lett.*, Vol. 11, 1307–1310, 2012.
9. Hubka, P. and J. Lacik, "X-band circularly polarized HMSIW U-slot antenna," *Radioengineering*, Vol. 25, No. 4, 687–692, 2016.
10. Liu, B., W. Hong, Y. Wang, Q. Lai, and K. Wu, "Half mode substrate integrated waveguide (HMSIW) 3-dB coupler," *IEEE Microw. Wireless Compon. Lett.*, Vol. 17, No. 1, 22–24, 2007.
11. Wang, Y., W. Hong, Y. Dong, B. Liu, H. G. Tang, J. Chen, X. Yin, and K. Wu, "Half mode substrate integrated waveguide (HMSIW) bandpass filter," *IEEE Microw. Wireless Compon. Lett.*, Vol. 17, No. 4, 265–267, 2007.
12. Jin, C., R. Li, A. Alphones, and X. Bao, "Quarter-mode substrate integrated waveguide and its application to antennas design," *IEEE Trans. Antennas Propag.*, Vol. 61, No. 6, 2921–2928, 2013.
13. Jin, C., Z. Shen, R. Li, and A. Alphones, "Compact circularly polarized antenna based on quarter-mode substrate integrated waveguide sub-array," *IEEE Trans. Antennas Propag.*, Vol. 62, No. 2, 963–967, 2014.

14. Moscato, S., C. Tomassoni, M. Bozzi, and L. Perregrini, "Quarter-mode cavity filters in substrate integrated waveguide technology," *IEEE Trans. on Microw. Theory Techn.*, Vol. 64, No. 8, 2538–2547, 2016.
15. Wang, N. and X. Xu, "A compact planar circularly polarized eighth-mode substrate integrated waveguide antenna," *International Journal of Microwave and Wireless Technologies*, 1–12, 2018.
16. Kim, K. and S. Lim, "Miniaturized circular polarized TE_{10} mode substrate-integrated-waveguide antenna," *IEEE Antennas Wireless Propag. Lett.*, Vol. 13, 658–661, 2014.
17. Jin, C. and Z. Shen, "Compact triple-mode filter based on quarter-mode substrate integrated waveguide," *IEEE Trans. Microw. Theory Techn.*, Vol. 62, No. 1, 37–45, 2014.
18. Balanis, C. A., *Antenna Theory: Analysis and Design*, Wiley, New Jersey, 2005.
19. Lai, Q., C. Fumeaux, W. Hong, and R. Vahldieck, "Characterization of the propagation properties of the half-mode substrate integrated waveguide," *IEEE Trans. Microw. Theory Techn.*, Vol. 57, No. 8, 1996–2004, 2009.
20. Xu, F. and K. Wu, "Guided-wave and leakage characteristics of substrate integrated waveguide," *IEEE Trans. Microw. Theory Techn.*, Vol. 53, No. 1, 66–72, 2005.